Supplementary Information

Supplementary Table 1. Summary of Rab antibodies

Rab antigen	Clonality	Dilution Ranges		Source
		I.B	I.F	
Rab1b	Rabbit (G-20)	1:200-1:500	1:50-1:200	Santa Cruz Biotechnology, Inc.
Rab2	Rabbit (FL-212)	1:200-1:500	1:50-1:200	Santa Cruz Biotechnology, Inc.
Rab3a/b/c	Mouse (42.1)	1:000-1:5000	1:500-1:2000	Synaptic Systems
Rab3a	Mouse (42.2)	1:1000-1:5000	1:500-1:2000	Synaptic Systems
Rab3b	Rabbit	1:300-1:500	1:100	(Schluter et al., 2002)
Rab3c	Rabbit	1:500-1:2000	1:500	Synaptic Systems
Rab4	Rabbit	1:1000	N/A	Abcam
Rab5	Mouse (621.3)	1:1000-1:2000	1:250-1:500	Synaptic Systems
Rab6	Rabbit	1:1000-1:5000	1:500	(Opdam et al., 2000)
Rab7	Rabbit (R8)	1:200-1:500	N/A	(Takamori et al., 2006)
Rab10	Rabbit	1:1000	N/A	ProteinTech Group, Inc
Rab11b	Goat (K-13)	1:200	N/A	Santa Cruz Biotechnology, Inc.
Rab14	Rabbit (H-55)	1:500	N/A	Santa Cruz Biotechnology, Inc.
Rab18	Rabbit	1:2000	N/A	Calbiochem
Rab27	Rabbit	1:500-1:1000	N/A	Synaptic Systems
Rab27a	Rabbit	1:500-1:1000	Not tested	Synaptic Systems
Rab27b	Rabbit	1:500-1:2000	1:100-1:500	Synaptic Systems
Rab27b	Rabbit	1:500-1:1000	1:50-1:200	(Barral et al., 2002)
Rab33b	Rabbit (RR-3)	1:200	N/A	Santa Cruz Biotechnology, Inc.
Rab34/39/Rah	Rabbit	1:200-1:500	N/A	ProteinTech Group, Inc
Rab35	Rabbit	1:800-1:2000	1:200	(Kouranti et al., 2006)

N/A= Not Applicable.

Supplementary Figure 1. (**a**) Overview of the SV isolation and purification protocol. (**b**) SV protein separation by SDS-PAGE. Shown is the 1-D separation of proteins from the various rat brain homogenates and CPG-purified SVs. Each fraction (5 μg of proteins) was separated on a 12.5% polyacrylamide gel and stained with Coomassie Brilliant Blue R-250. Arrow corresponds to the predicted migration of synaptophysin (Syph) (**c**) Immunoblot assessment of SV enrichment using antibodies against SV markers Syph and synaptobrevin (Sybrv), and post-synaptic marker NMDA-receptor (NMDAR).

Supplementary Figure 2. (**a**) Phylogenetic tree of rat Rab GTPases. The tree was generated as described in the Supplementary Material and Methods. The labels on the tree edges represent the likelihood mapping (LM) (first) and almost unbiased (AU) support values (right). (**b**) Characterization of Rab3a and Rab27b antibodies. The indicated EGFP-Rab proteins were transfected in HEK293 cells. After 48hrs, the cells were lysed and proteins (10 μg) were resolved by 12.5% SDS-PAGE before being transferred to nitrocellulose and probed with antibodies against Rab3a (monoclonal, Cl 42.2) or Rab27b (polyclonal, Synaptic Systems, Germany).

Supplementary Figure 3. Localization of EGFP constructs in hippocampal neurons. Hippocampal neurons were transfected 8-10 DIV with the indicated EGFP constructs and fixed 48 hours post-transfection before being examined for EGFP signal by fluorescence microscopy. Note that EGFP-Rab1b and -Rab6b are largely associated with a reticular perinuclear structure reminiscent of the Golgi. EGFP-Rab3a, -Rab27b are almost exclusively targeted to synaptic boutons lining along neuronal axons. EGFP-Rab4b, -Rab5a, -Rab10, -Rab11b and -Rab14 also display select localization to synaptic boutons as well as clear perinuclear endosome-like signal. Bar, 20 μm.

Supplementary Figure 4. Localization of endogenous Rabs in hippocampal neurons. Neuronal cultures (17 DIV) were fixed with 3% PFA (Rabs 1b, -2, -6) or methanol (Rab5) and triple-labeled with endogenous antibodies against the indicated Rab in combination with either synaptophysin (Syph)/GM130 (Golgi marker) or synph/Rab3a. Yellow arrowheads correspond to triple-colocalized punctae, white arrowheads denote Rab5-only labeled punctae. Bar, 10 μm.

Supplementary Figure 5. Rab3a and Rab27b displays local axonal movement in hippocampal neurons. (**a**) EGFP-Rab27b and mRFP-Rab3a colocalize largely to immobile synaptic boutons in neuronal axons. Shown are individual frames from an epifluorescence time series displaying dual-positive EGFP-Rab27b and mRFP-Rab3a labeled compartments in an axon of a rat hippocampal neuron (**b**) and the corresponding kymograph (**c**). Arrows indicate moving carriers and dotted lines indicate two examples of oscillating EGFP-Rab27b/mRFP-Rab3a punctae. Asterisks denote stationary boutons. The hippocampal soma is out of view to the left. See also Supplementary Video1. Bar, 10 μm (**a,c**) and 5 μm (**b**).

Supplementary Figure 6. Overexpression of EGFP-Rab27b wild-type and mutant fusion chimeras does not alter dendrite morphology and outgrowth in rat hippocampal neurons. (**a,b**) Neurons (10 DIV) were transfected as detailed in the Materials and Methods with the indicated EGFP-Rab27 constructs and fixed in 3% PFA 48hrs post-transfection. Dendritic processes were stained for the somatodendritic marker MAP2 (blue) and representative images are shown. Only MAP2-positive processes were counted as dendrites. No obvious difference in dendritic morphology and number is observed between Rab27b wt and mutant transfected hippocampal neurons. Data represent means ± s.e.m. (n=17-25 cells per group). Bar, 10 μm. (**c**) Morphology and density of synaptic boutons in rat hippocampal neurons (13 DIV) expressing EGFP-Rab27bwt and mutant fusion chimeras. Transfected neurons were stained with synaptophysin

(Syph) to visualize synaptic boutons (**c**) and bouton density calculated by counting the number of boutons/axon length (**d**). No significant differences in synaptic densities were observed between EGFP-Rab27bwt and mutant neurons. Data represent means ± s.e.m. (n = 150-200 boutons analyzed per group). Bar, 5 µm

Supplementary Figure 7. FM4-64FX loading and release in rat hippocampal neurons overexpressing EGFP-Rab27bwt. (a) Schematic overview of the FM4-64FX loading and destaining protocol. Neurons (10 DIV) grown on coverslips were transiently transfected with 10 µg of plasmid encoding EGFP-Rab27wt. After 48 hrs, cells were transferred to stimulating media (neuronal buffer + 50 mM KCl) containing FM4-64FX (10 µm) for 90 sec to ensure completion of endocytosis and loading of rapidly recycling synaptic vesicles. Following extensive washing (10 min), FM4-64FX-loaded neurons were subjected to a second round of stimulation (high K^+ solution), fixed 10 min post-stimulation, and FM4-64FX release assessed by fluorescence microscopy (b). Representative images of EGFP-Rab27bwt-labeled boutons (green) and their corresponding FM4-64FX images (red) are shown along with the pseudocolor merge. Note that the level of co-localized EGFP/FM4-64FX signal (yellow color in merge) is markedly reduced following a second round of stimulation and destaining.

Supplementary Video 1. The video shows mRFP-Rab3a (red) and EGFP-Rab27b (green) in the axon of a rat hippocampal neuron 36 hours after transfection. Images were acquired at 5-second intervals at 37°C on a temperature controlled stage. We observed occasional single-labeled EGFP-Rab27b and mRFP-Rab3a compartments moving in and out of synaptic boutons or merging as single entities. However, no long-range movements of EGFP-Rab27b or mRFP-Rab3a compartments were observed in axons imaged within the resolution constraints of the microscope setup. Speed is 10 times actual.

Supplementary Methods

Bioinformatics and phyogenetic tree construction

All Rab sequences were collected from the NCBI protein database from the National Center for Biotechnology Information (NCBI; www.ncbi.nlm.nih.gov) and aligned using muscle(Edgar, 2004) and optimized by hand. The phylogenetic reconstruction was composed of two different analytical approaches. The first approach used IQPNNI (Important Quartet Puzzling and Nearest Neighbor Interchange) (Vinh le, 2004) to construct phylogenetic trees from the curated alignments. We used a gamma distribution as a model for rate heterogeneity with four rate

categories for the estimation of the gamma distribution parameter. The proportion of invariable sites was estimated from the data and the Jones, Taylor and Thornton (JTT-) distance matrix (Jones et al., 1992) served as a substitution matrix. We used the stopping rule of IQPNNI, but the calculation had to run for at least the suggested number of iterations. The default values were used for the remaining parameter. In addition, Likelihood-Mapping (LM) was applied to determine the confidence of the edges in the calculated trees. The second approach used the phylib package (Felsenstein, 1989) to apply a distance-based bootstrap analysis with 1000 replicates to each of the curated alignments. Standard settings were used for seqboot, the JTT distance matrix and also a gamma distribution (with parameter approximation from tree-puzzle) for protdist, as were standard options for neighbour. If required, the random seed was set to nine. We used the almost unbiased (AU) test (Shimodaira, 2002) to address the systematically biased bootstrap values. We obtained the sitewise log-likelihoods needed for the AU test using a modified version of phyml (Guindon and Gascuel, 2003) and the test was performed using consel (Shimodaira and Hasegawa, 2001). The reconstructed IQPNNI trees served as starting points to join the results of both calculations. The inner edges of the trees were labeled with their LM and corrected bootstrap support values.

Analysis of dendritic growth and synaptic density

Cultured hippocampal neurons (8-10 DIV) grown in neurobasal medium containing B27 supplements were transiently transfected with 10 µg of plasmid encoding EGFP-Rab27wt and mutant fusions using the Profection® mammalian transfection system-calcium phosphate (Promega, Madison, WI) . Forty-eight hours post-transfection, cells were fixed with 3% PFA and stained with either mouse anti-MAP2 (1:3,000, Synaptic Systems) or synaptophysin (1:10,000, Synaptic Systems). Images were acquired with an epifluorescence microscope (Axiovert 200M; Carl Zeiss MicroImaging, Inc.) with either a 40x (NA 1.2) or 63x (NA 1.4) plan Apochromat oil immersion objective (Carl Zeiss MicroImaging, Inc.), standard filter sets (Carl Zeiss MicroImaging, Inc.), a 1,317 x 1,035-pixel cooled CCD camera (Princeton Instruments), and Metamorph software (Metamorph Inc). The numbers of MAP2-positive dendrites per neuron and synaptophysin-labeled synaptic boutons were quantified using NeuronJ and ImageJ macros (NIH).

Supplementary References

Barral DC, Ramalho JS, Anders R, Hume AN, Knapton HJ, Tolmachova T, Collinson LM, Goulding D, Authi KS, Seabra MC (2002) Functional redundancy of Rab27 proteins and the pathogenesis of Griscelli syndrome. J Clin Invest 110:247-257.

Edgar RC (2004) MUSCLE: a multiple sequence alignment method with reduced time and space complexity. BMC Bioinformatics 5:113.

Felsenstein J (1989) PHYLIP-Phylogeny Inference Package (Version 3.2). Cladistics 5:164 -166.

Guindon S, Gascuel O (2003) A simple, fast, and accurate algorithm to estimate large phylogenies by maximum likelihood. Syst Biol 52:696-704.

Jones DT, Taylor WR, Thornton JM (1992) The rapid generation of mutation data matrices from protein sequences. Comput Appl Biosci 8:275-282.

Kouranti I, Sachse M, Arouche N, Goud B, Echard A (2006) Rab35 regulates an endocytic recycling pathway essential for the terminal steps of cytokinesis. Curr Biol 16:1719-1725.

Opdam FJ, Echard A, Croes HJ, van den Hurk JA, van de Vorstenbosch RA, Ginsel LA, Goud B, Fransen JA (2000) The small GTPase Rab6B, a novel Rab6 subfamily member, is cell-type specifically expressed and localised to the Golgi apparatus. J Cell Sci 113 (Pt 15):2725-2735.

Schluter OM, Khvotchev M, Jahn R, Sudhof TC (2002) Localization versus function of Rab3 proteins. Evidence for a common regulatory role in controlling fusion. J Biol Chem 277:40919-40929.

Shimodaira H (2002) An approximately unbiased test of phylogenetic tree selection. Syst Biol 51:492-508.

Shimodaira H, Hasegawa M (2001) CONSEL: for assessing the confidence of phylogenetic tree selection. Bioinformatics 17:1246-1247.

Takamori S et al. (2006) Molecular anatomy of a trafficking organelle. Cell 127:831-846.

Vinh le S, and Von Haeseler, A (2004) IQPNNI: moving fast through tree space and stopping in time. Mol Biol Evol 21:1565-1571.

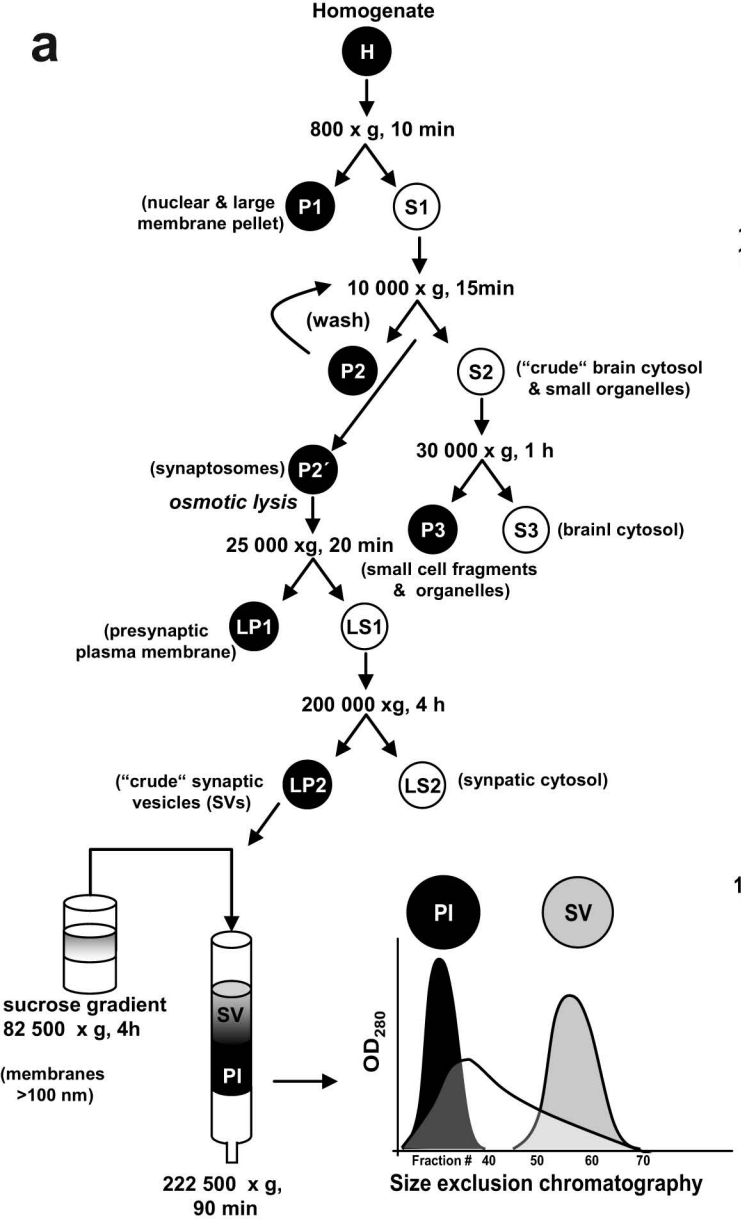

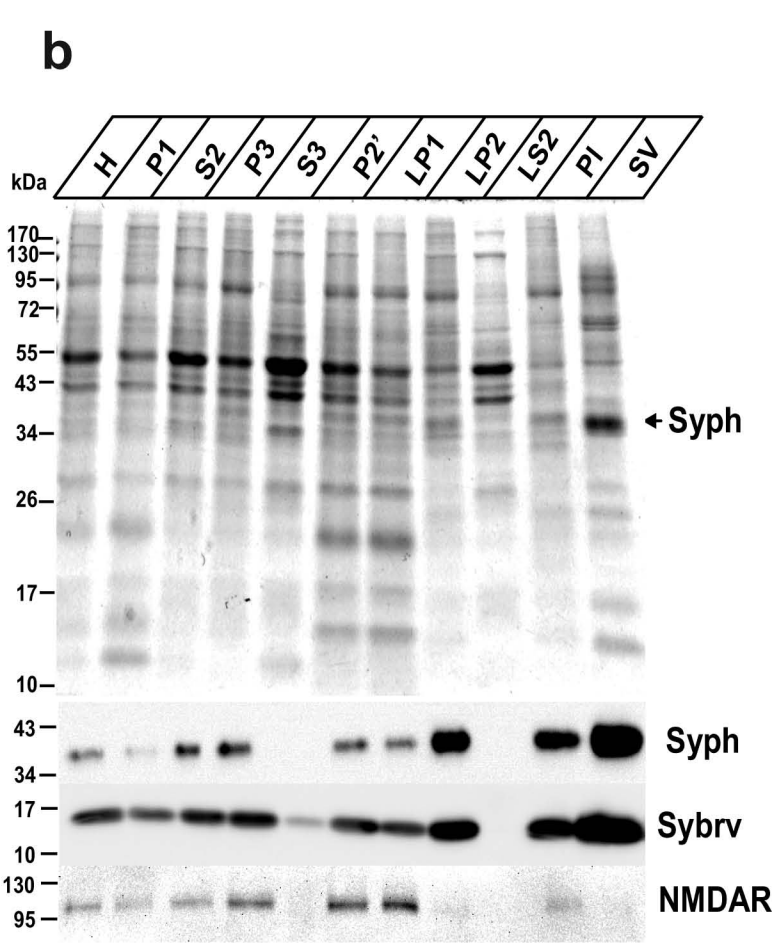

Supplementary Figure 1

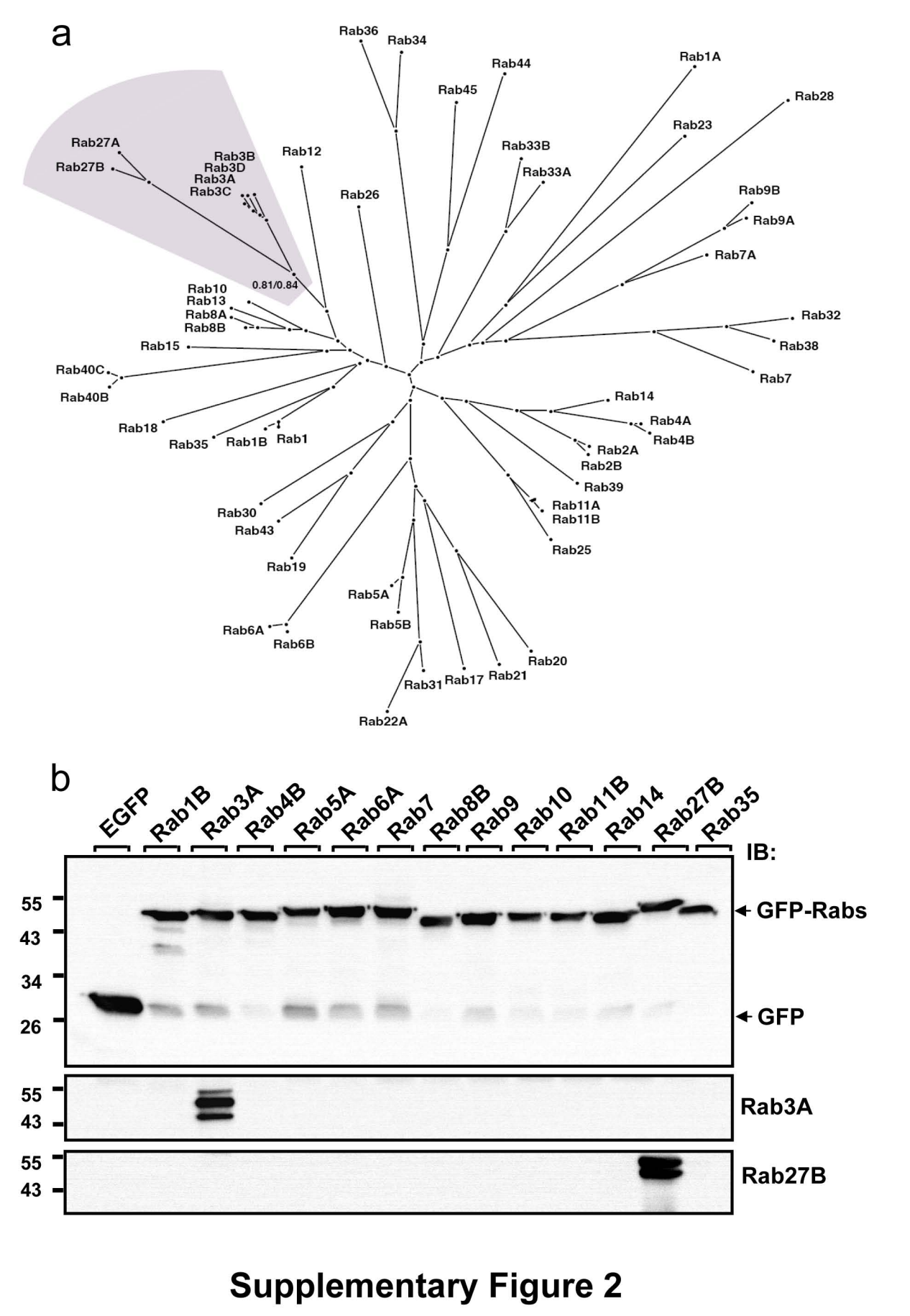

Supplementary Figure 2

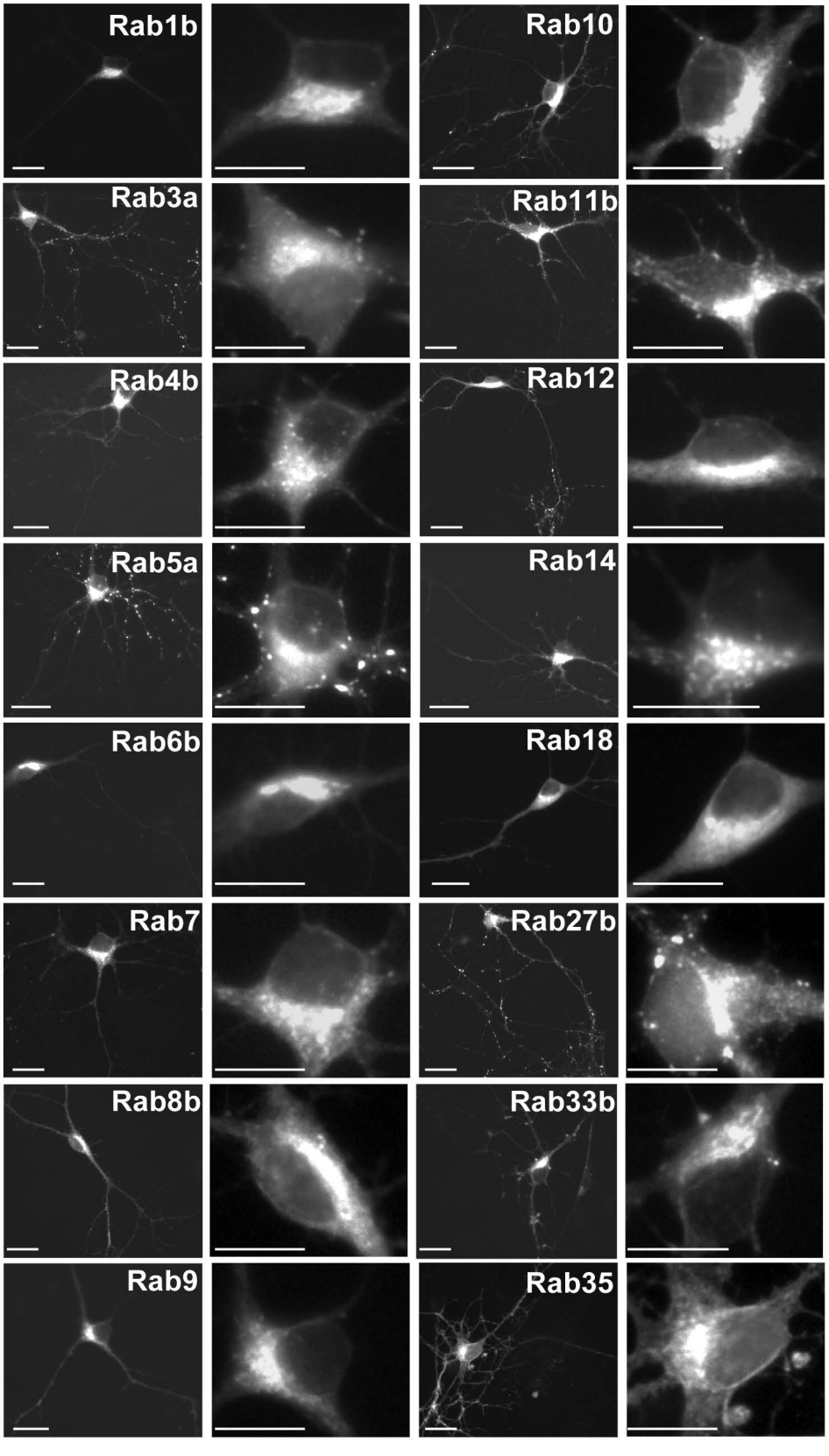

Supplementary Figure 3

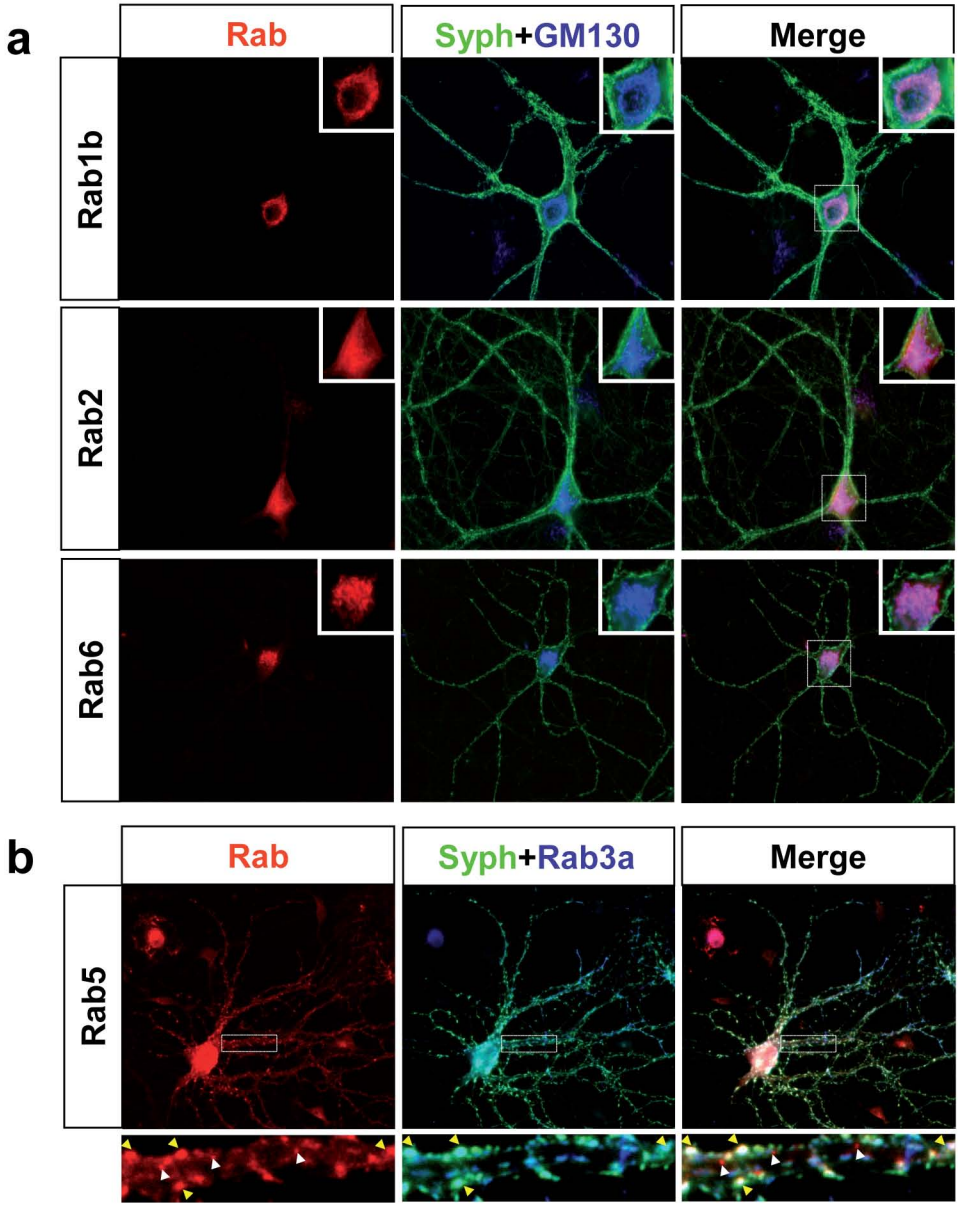

Supplementary Figure 4

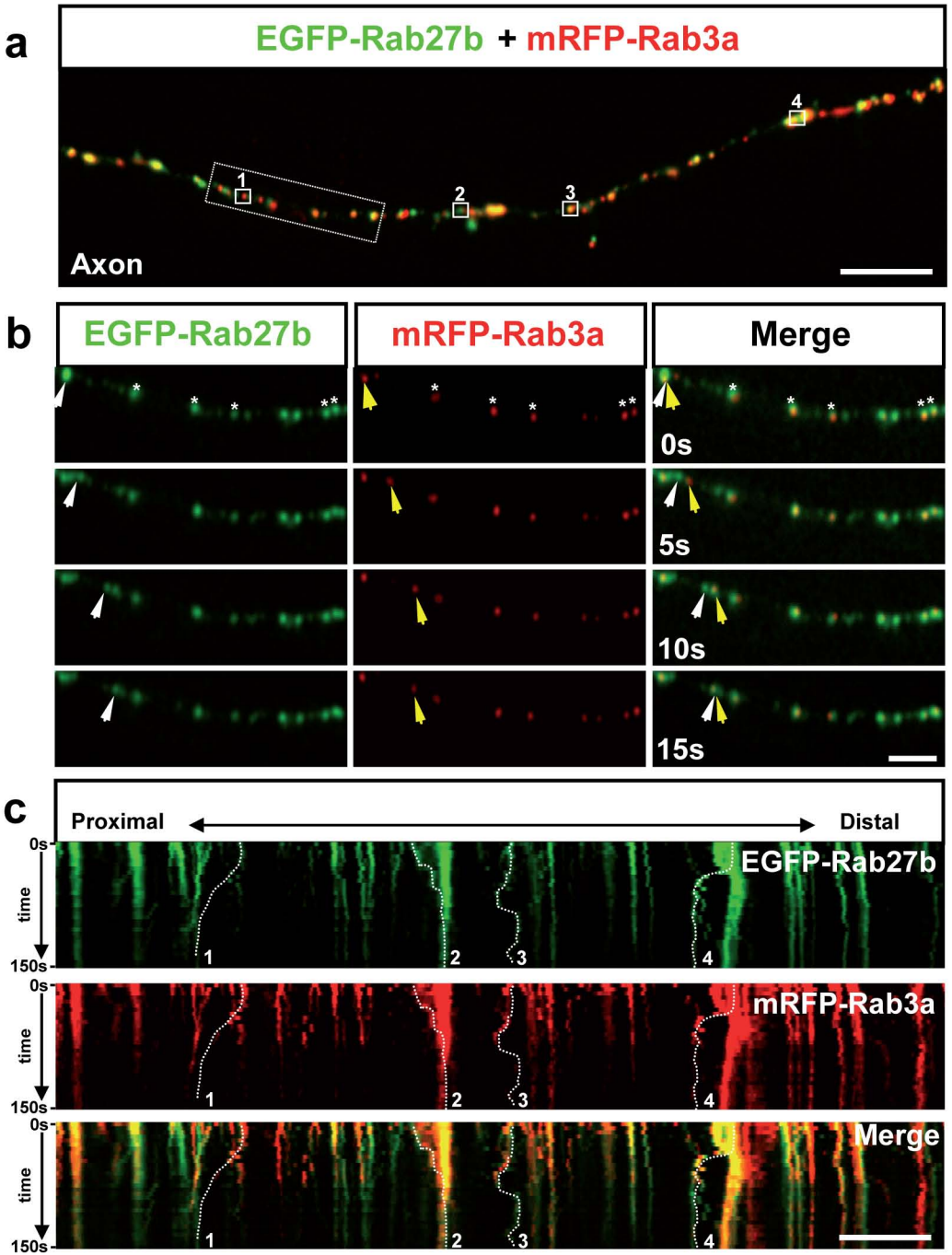

Supplementary Figure 5

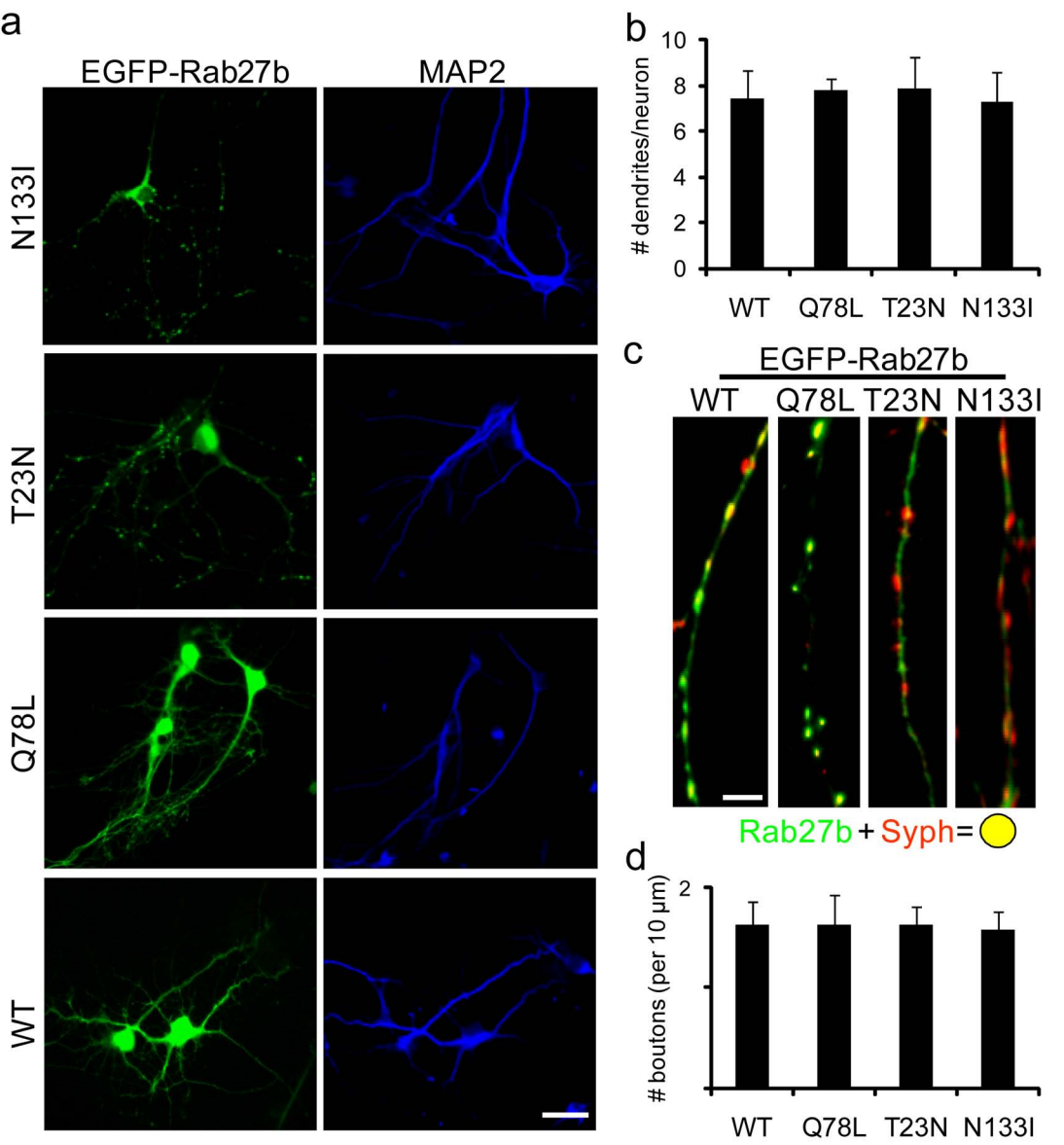

Supplementary Figure 6

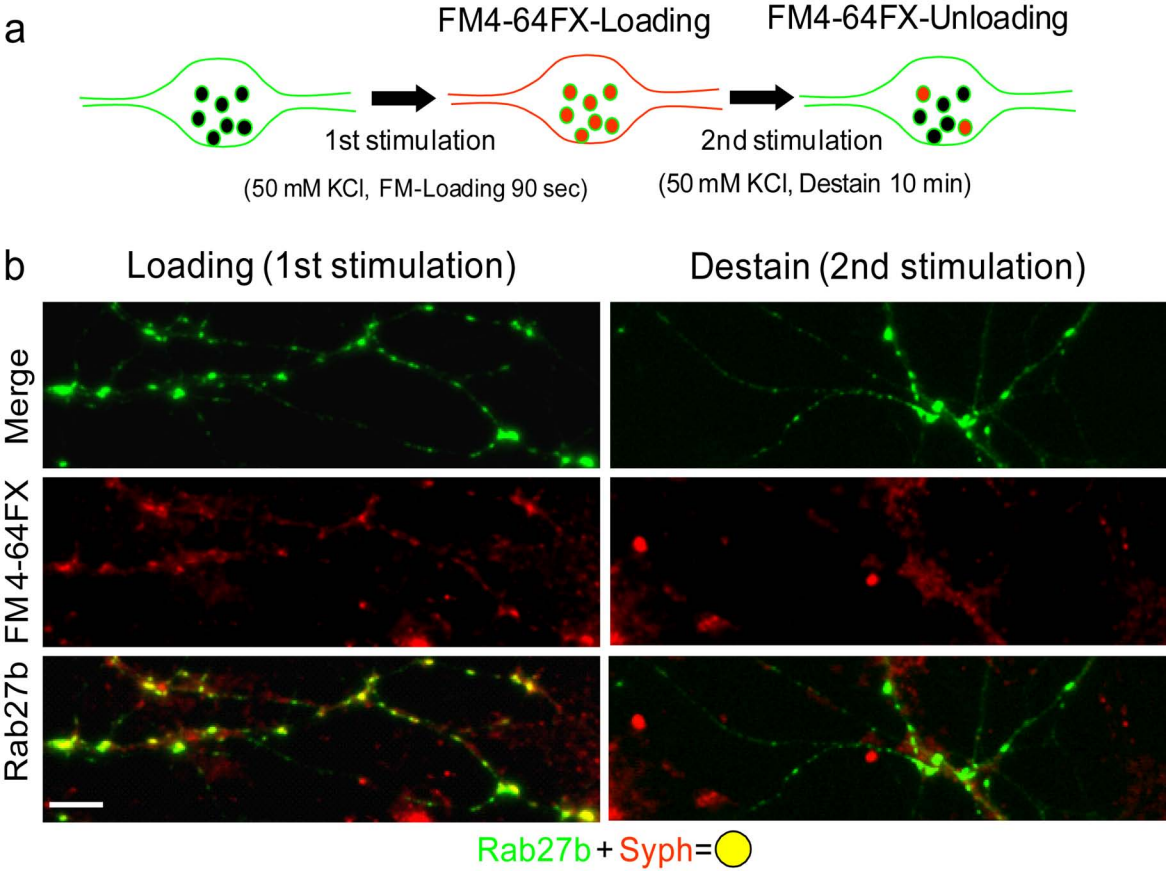

Supplementary Figure 7